# Embedded controller optimization for efficient electric motor drive

Hiba Houmsi, Paolo Massioni, Federico Bribiesca Argomedo, Romain Delpoux

# Embedded controller optimization for efficient electric motor drive

Hiba Houmsi
*Univ Lyon, INSA Lyon,*
*Université Claude Bernard Lyon 1,*
*Ecole Centrale de Lyon,*
*CNRS, Ampère, UMR5005*
69621 Villeurbanne, France
hiba.houmsi@insa-lyon.fr

Paolo Massioni
*Univ Lyon, INSA Lyon,*
*Université Claude Bernard Lyon 1,*
*Ecole Centrale de Lyon,*
*CNRS, Ampère, UMR5005*
69621 Villeurbanne, France
paolo.massioni@insa-lyon.fr

Federico Bribiesca-Argomedo
*Univ Lyon, INSA Lyon,*
*Université Claude Bernard Lyon 1,*
*Ecole Centrale de Lyon,*
*CNRS, Ampère, UMR5005*
69621 Villeurbanne, France
federico.bribiesca-argomedo@insa-lyon.fr

Romain Delpoux
*Univ Lyon, INSA Lyon,*
*Université Claude Bernard Lyon 1,*
*Ecole Centrale de Lyon,*
*CNRS, Ampère, UMR5005*
69621 Villeurbanne, France
romain.delpoux@insa-lyon.fr

***Abstract*—This article proposes an approach that aims to reduce the gap between control theory and its use in industrial practice, in particular in electric motor drives. We explore means to embed optimal control methods based on convex optimization directly into microcontrollers, in order to be able to recompute or update the control law regularly without the need of external intervention of an expert. This has been made possible by running a real-time scheduler on the microcontroller which can run two tasks, a fast task consisting of the motor drive control law, and a low-priority task containing the optimization solver. A simple, targeted, Linear Matrix Inequality (LMI) solver has been developed for this scope. The feasibility of this approach is demonstrated through a set of experimental results.**

***Index Terms*—Motor drive, embedded control, Linear Matrix Inequalities (LMIs).**

## I. Introduction

Electromobility is a critical aspect of the automotive industry, where robustness and performance are required. Permanent Magnet Synchronous Motors (PMSMs) exhibit those qualities due to high power density, ease to manufacture and compact structure [1]. To enhance the efficiency of the energy conversion system and to take advantage of the intrinsic characteristics of the PMSM, researchers have extensively explored various feedback controllers, such as cascaded Proportional-Integral (PI) controllers [2], model predictive control [3], linear-quadratic regulator [4], etc. Cascaded speed and current PI controllers have been historically used since the discovery of Park and Clarke's transformations [5], and they are tuned most of the time with pole placement methods (Ackerman's formula) [2]. Model predictive control and linear quadratic regulators are optimization-based controllers that require user-defined matrices in order to introduce a trade-off between power consumption and performance in a system. In [4], these matrices are used to compute offline the gain of a state feedback controller.

In most of the aforementioned methods, controller gain tuning is a non-trivial task, where the user is required to set a specific value for the poles or the cost functions, rather than an acceptable range of values. The robust pole placement Linear Matrix Inequalities (LMIs) regions method presented in [6] is very interesting in this perspective, as it allows one to just set an acceptable desired region of the complex plane for the closed loop poles; this relieves the user from the burden of precise control tuning, still ensuring the stability and performance of the controlled system. This method has been applied offline, for example in [7], in order to control an integrated Light-Emitting Diode (LED) driver. The same approach is used in [8] to drive a magnetic levitation plant and in [9] to drive a PMSM.

Focusing on PMSMs, they are nonlinear systems with fast dynamics; this often discourages the use of convex optimization-based controllers for embedded applications. This paper's contribution is to introduce an alternative approach featuring an onboard LMI feasibility problem solver to synthesize controllers, based on a computationally efficient implementation of an interior-point method algorithm. This embedded optimization process is capable of finding a controller that fulfills a given set of specification, namely it imposes a minimum decay rate and a minimum acceptable damping for the closed-loop poles. This onboard approach has several advantages, such as the ability to reconfigure the controller without requiring an expert operator and a lightweight algorithm that is suitable for small, budget-friendly

microcontrollers. To the best of our knowledge, this is the first time that this strategy has been proposed and experimentally validated on an industrial microcontroller, specifically the ATSAME54P20A. The results of the experiment are promising for on-chip industrial applications.

This paper is organized as follows: Section II first presents the PMSM model, the regional pole placement method and the interior-point LMI solver that we employ. Subsequently, Section III describes the embedded control scheme as well as its implementation on an industrial microcontroller, providing also some experimental results. Section IV concludes the paper, with a summary of the contributions and outlines for future research directions.

## II. Preliminaries

### A. Notation

We denote by $\mathbb{R}$ the set of real numbers and by $\mathbb{R}^{n\times m}$ the set of real $n \times m$ matrices. $A^\top$ indicates the transpose of a matrix $A$, $I$ is the identity matrix. The notation $A \succ 0$ (resp. $A \prec 0$) indicates that all the eigenvalues of the symmetric matrix $A$ are strictly positive (resp. negative). The imaginary part of a complex number $z$ is denoted $\Im(z)$ and the real part $\Re(z)$. Last, the notation $[v; w]$ indicates the column concatenation of two column vectors or scalars.

### B. Electric motor model

Using Clarke and Park's transformations [10], the Surface-Mounted Permanent Magnet Synchronous Motor (SPMSM) mathematical model in the d-q frame is expressed as:

$$\begin{cases} L\frac{di_d}{dt} = v_d - Ri_d + pL\omega i_q, \\ L\frac{di_q}{dt} = v_q - Ri_q - pL\omega i_d - p\phi_f\omega, \\ J\frac{d\omega}{dt} = \frac{3}{2}p\phi_f i_q - f\omega - \tau_l; \end{cases} \tag{1}$$

where the inputs of the system are $v_d$, $v_q$, the d-q phase voltages and the measured states of the system are $i_d$, $i_q$ and $\omega$ respectively the d-q phase currents and rotor angular speed, $R$ the phase resistance, $L$ the phase inductance, $\phi_f$ the peak magnetic flux of the permanent magnets seen by stator windings, $p$ the pole pairs number, $J$ the inertia of the system, $f$ is the viscous frictional coefficient of the motor, $\tau_l$ the load torque considered as an exogenous disturbance (not measured). The system described in (1) is nonlinear due to the product of two state variables, so a feedback linearization method is applied to eliminate these nonlinear terms [11]. Choosing:

$$\begin{cases} v_d = u_d - pL\omega i_q, \\ v_q = u_q + pL\omega i_d, \end{cases} \tag{2}$$

the system (1) can be then rewritten as:

$$L\frac{di_d}{dt} = u_d - Ri_d; \tag{3a}$$

$$L\frac{di_q}{dt} = u_q - Ri_q - p\phi_f\omega, \tag{3b}$$

$$J\frac{d\omega}{dt} = \frac{3}{2}p\phi_f i_q - f\omega - \tau_l; \tag{3c}$$

One can split this system into two independent linear time-invariant systems: a first-order system that characterizes $i_d$ dynamic, and a second-order system that describes $i_q$ and $\omega$ dynamics. A controller is built for each subsystem and, to ensure zero steady state error in the presence of constant disturbances and parameter mismatch, the state space model is augmented with an integral action. Using [12], the tracking error can be defined as:

$$\dot{e}_i = \begin{bmatrix} -\frac{R}{L} & 0 \\ 1 & 0 \end{bmatrix} e_i + \begin{bmatrix} \frac{1}{L} \\ 0 \end{bmatrix} u_d \tag{4}$$

where $e_i = \begin{bmatrix} i_d - i_d^\# & \varepsilon_i \end{bmatrix}$ and $\varepsilon_i = \int_0^t (i_d - i_d^\#)dt$ the integral action over the output of the system $\varepsilon_i$. The tracking error state space model of the $i_q$ and $\omega$ dynamic [12]:

$$\dot{e}_\omega = \begin{bmatrix} -\frac{R}{L} & \frac{p\phi_f}{L} & 0 \\ \frac{3p\phi_f}{2J} & \frac{-f}{J} & 0 \\ 0 & -1 & 0 \end{bmatrix} e_\omega + \begin{bmatrix} \frac{1}{L} \\ 0 \\ 0 \end{bmatrix} u_q \tag{5}$$

where $e_\omega = \begin{bmatrix} i_q & \omega - \omega^\# & \varepsilon_\omega \end{bmatrix}$ and $\varepsilon_\omega = \int_0^t (\omega - \omega^\#)dt$ the integral action over the output of the system $\varepsilon_\omega$. Both models (4) and (5) can be written in the classical state-space form:

$$\dot{x}(t) = Ax(t) + Bu(t) \tag{6}$$

with $x \in \mathbb{R}^n$, $u \in \mathbb{R}^m$ and with appropriate definitions of $n$, $m$, $x(t)$, $u(t)$, $A$ and $B$. The primary objective of a control system is then to guarantee stability and performance when subject to unknown disturbances and parametric variation. Ultimately, this involves determining the state-feedback gain $K$ for the control law:

$$u(t) = Kx(t) \tag{7}$$

in a way that, when such a control is applied, the closed-loop system in the following form:

$$\dot{x}(t) = (A + BK)x(t) \tag{8}$$

possesses the desired properties.

### C. Regional pole placement

This subsection provides a synthesis of how a resilient pole placement via LMIs [6] can be utilized to synthesize the full-feedback gain matrix (7). The goals are the following:

(i) the closed-loop dynamics has to be asymptotically stable (i.e., the error converges to zero),
(ii) the closed-loop poles should guarantee an exponential decay rate $\alpha$ within a minimum $\alpha_{min}$ and maximum $\alpha_{max}$ values,
(iii) the damping factor of the system $z$ should be greater than a minimum specified value $z \geqslant \frac{1}{\sqrt{1+\beta^2}}$ expressed in terms of a positive tuning parameter $\beta$.

Figure 1 depicts the constraints $\alpha_{min}$, $\alpha_{max}$ and $\beta$ over the real and imaginary parts of the eigenvalues of the closed-loop system.

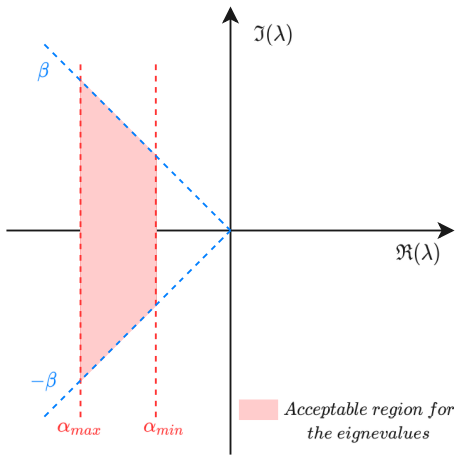


Fig. 1: Acceptable region for the eigenvalues of the closed-loop system according to the constraints $\alpha$ and $\beta$.

Finding a controller gain matrix $K$ that satisfies these specifications boils down to the following LMI feasibility problem:

$$\underset{x}{\text{find}}\ L \in \mathbb{R}^{m\times n},\ X = X^\top \in \mathbb{R}^{n\times n}\ \text{s.t.} \tag{9a}$$

$$H_1 = X \succ 0 \tag{9b}$$

$$-H_2 = XA^\top + L^\top B^\top + AX + BL + 2X\alpha_{min} \prec 0 \tag{9c}$$

$$H_3 = XA^\top + L^\top B^\top + AX + BL + 2X\alpha_{max} \succ 0 \tag{9d}$$

$$-H_4 = \begin{bmatrix} \beta(XA^\top + L^\top B^\top + AX + BL) & AX + BL - XA^\top - L^\top B^\top \\ XA^\top + L^\top B^\top - AX - BL & \beta(XA^\top + L^\top B^\top + AX + BL) \end{bmatrix} \prec 0 \tag{9e}$$

With an affine parameterization of $X$, $L$ as $X(\xi)$, $L(\xi)$ where $\xi \in \mathbb{R}^\mu$, is a vector of decision variables, with $\mu = \frac{n(n+1)}{2} + n\times m$. This problem can be solved with standard semidefinite programming constrained optimization methods, and the controller can then be retrieved with the transformation

$$K = LX^{-1}.$$

Notice that the existence of a solution for the problem above is a sufficient condition for the existence of a controller that successfully places the poles in the desired area, but not necessary. This is due to the *conservatism* involved in the convexification of the problem, see again [6] for details.

### D. Interior point solver

Feasibility problem (9a)-(9e) can be solved by means of an interior point algorithm, whose working principle is based on turning the constrained optimization into an unconstrained one, on which Newton iterations can be applied [13]. This conversion is obtained through the use of an augmented cost function that includes a barrier function, i.e., a term going to infinity when the edge of the constrained region is approached.

The equations of problem (9a)-(9e) can be put in a single inequality as

$$F = \begin{bmatrix} H_1 & 0 & 0 & 0 \\ 0 & H_2 & 0 & 0 \\ 0 & 0 & H_3 & 0 \\ 0 & 0 & 0 & H_4 \end{bmatrix} \succ 0 \tag{10}$$

where $F$ is a symmetric matrix affine in the unknowns $\xi$, i.e.:

$$F(\xi) = F_0 + \sum_{i=1}^{\mu} \xi_i F_i \tag{11}$$

where $F_i$ are constant, symmetric matrices. Problem (9a)-(9e) is then equivalent to finding a value $\xi^\star$ of $\xi$, for which

$$F(\xi^\star) \succ 0, \tag{12}$$

which is also equivalent to finding values $\xi^*$, $\lambda^* < 0$ for which

$$F(\xi^*) + \lambda^* I \succ 0. \tag{13}$$

Notice that for the problem in this last formulation, it is always possible to find a simple feasible starting point (a set of $\xi$, $\lambda$ for which the inequality is satisfied) by simply taking $\xi = 0$, and $\lambda > -\underline{\lambda}(F_0)$, with $\underline{\lambda}(F_0)$ the minimum eigenvalue of $F_0$. The interior point algorithm that we use is summarized here.

**Algorithm 1** Interior-point method

**Initialization**: set $\xi = 0$, $\lambda > -\underline{\lambda}(F_0)$, $l > \lambda$, set a $\theta \in (0,1)$, set a small tolerance $\varepsilon > 0$; define $\zeta = [\lambda;\ \xi]$, $\mathcal{F}(\zeta) = F(\xi) + \lambda I$.

**Execute**:

1) Define $\phi(\zeta)$ as $\phi(\zeta) = -\log\det(\mathcal{F}(\zeta)) - \log(l - \lambda)$.
2) Find $\zeta_c = [\lambda_c;\ \xi_c] = \arg\min \phi(\zeta)$ using an unconstrained optimization solver (Newton's method) and using $\zeta$ as starting point.
3) **If** $||\zeta - \zeta_c|| < \varepsilon$ or $\lambda < -\varepsilon$
   **then** $\zeta^* = [\lambda^*;\ \xi^*] \leftarrow \zeta_c$ and terminate;
   **otherwise** set $l \leftarrow \theta\lambda + (1-\theta)\lambda_c$, $\zeta \leftarrow \zeta_c$, go to 1.

**Outcome**: if $\lambda^* \geqslant 0$ the problem is infeasible, otherwise it is feasible and the controller gain can be retrieved as $K = L(\xi^*)X(\xi^*)^{-1}$.

The barrier term in this algorithm is minus the logarithm of the determinant of $\mathcal{F}$, which goes to plus infinity if one of the eigenvalues of $\mathcal{F}$ goes to zero, assuring that the algorithm never exits the $\mathcal{F}(\zeta) \succ 0$ zone as it is initialized inside it.

## III. Embedded motor drive

### A. Design of the control structure

In this subsection, we detail the control law implemented in the microcontroller. We utilize the embedded optimal pole placement method presented in subsection II-C and II-D to synthesize the state feedback gain $K_q$ for (5), with $x = e_\omega = \begin{bmatrix} i_q & \omega - \omega^\# & \varepsilon_\omega \end{bmatrix}^\top$, $u = u_q$. The focus of our discussion is limited to the controller of model (5), however, the same approach can be applied to synthesize a controller for (4).

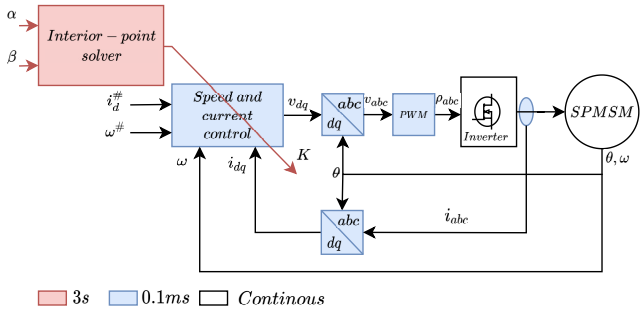


Fig. 2: Control scheme, with $K = [K_d : K_q]$.

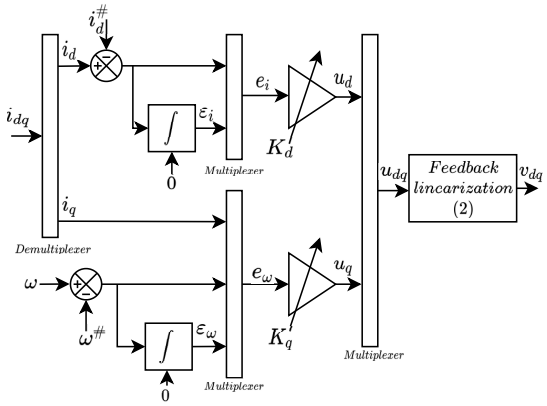


Fig. 3: Speed and current controller.

Figure 2 depicts the embedded control scheme as an input-output diagram. Using the desired values of $\alpha_{min}$, $\alpha_{max}$, and $\beta$ as input parameters, the interior-point solver block runs Algorithm 1 to solve the LMI feasibility problem. Thus, finding a state feedback matrix $K_q$ that satisfies the three goals detailed in II-C. On the other hand, Fig. 3 describes the speed and current control block. This block takes the measured states, references, and $K_q$ as inputs, and computes the $u_{dq}$ voltages. To obtain the d-q voltages $v_{dq}$ applied to the SPMSM from $u_{dq}$, feedback linearization (2) is used. The d-q frame is then transformed into the (a, b, c) frame using the Park and Clarke transformations [10]. Finally, Pulse-Width Modulation (PWM) is then used to drive the inverter. The interior-point solver (pink) and control task (blue), in Fig. 2, are executed respectively every $T_{solver} = 3$ [s] and $T_{ctrl} = 0.1$ [ms].

### *B. Experimental results*

To verify the practical applicability of the proposed approach in an industrial setting, we carried out experimental tests on a 3-phase SPMSM. The identified parameters of the SPMSM are listed in Tab. I, which were obtained using [14]. To perform the experiments, an embedded inverter demo-board from Microchip (MCLV-2) and an ATSAME54P20A 32-bit microcontroller were used (Tab. II provides further details). The real-time software was developed using a high-level rapid control prototyping solution, specifically, Matlab/Simulink [15]. Figure 4 shows the experimental setup.

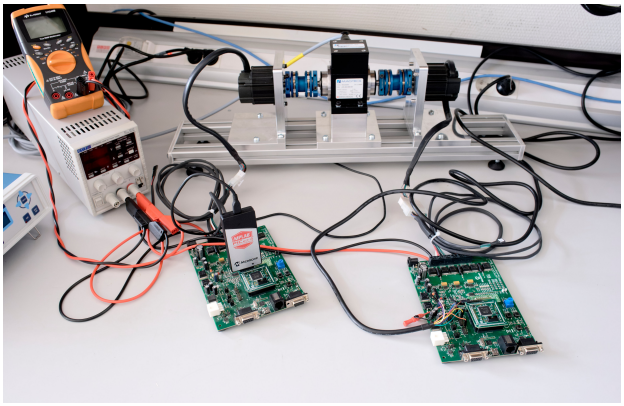

Fig. 4: PMSM and microcontroller-based electronics.

TABLE I: PMSM parameters.

| PMSM Parameters | Values | Units |
|---|---|---|
| $R$ | 0.656 | $\Omega$ |
| $L$ | 0.35 | mH |
| $\phi_f$ | 6.6 | mWb |
| $p$ | 4 | - |
| $f$ | $10^{-5}$ | kg m$^2$ |
| $J$ | $10^{-5}$ | N m s rad$^{-1}$ |
| $V_{dc}$ | 24 | V |

TABLE II: Some features of the ATSAME54P20A.

| Characteristic | Value |
|---|---|
| Architecture | 32-bit ARM Cortex-M4 |
| CPU speed (MIPS) | 120 |
| Size of programmable memory | 1024 |
| ADC | 12 bits |
| Floating point unit | yes |
| Unit price | 7.39 € |

We conducted experiments to test the control using a speed step from 100 rad/s to 200 rad/s with varying constraints $\alpha_{min}$, $\alpha_{max}$, and $\beta$. To simplify the analysis, we assume that $\alpha_{min}$ is equal to $\alpha$, and $\alpha_{max}$ is equal to $3\alpha$. For different values of $(\alpha, \beta)$, Fig. 5, displays the eigenvalues obtained by solving the LMI feasibility problem using algorithm 1. The speed response for each set of constraints, $(\alpha, \beta)$, is presented in Fig. 6. The figure highlights that increasing the value of $\alpha$ leads to more negative eigenvalues and faster speed response. Additionally, by allowing more oscillations through an increase in $\beta$, the speed response becomes faster, although it may exceed the reference during the transient. The actuator effort, is depicted in Fig. 7 to insure the system is not saturated. Choosing $\alpha_{max}$ is important to avoid very fast eigenvalues and prevent the system from exceeding certain physical or operational limits.

In this experiment, the microcontroller performs all the computations, and requires 2.344 seconds to solve the low priority LMI feasibility problem. During these 2.344 seconds, the processor is pre-empted every $T_{ctrl}$ to perform the high priority motor control task before going back to the low priority task. This interruption is done following a rate-monotonic scheduling policy, which ensures that the high priority task is

always executed, regardless of the microcontroller's workload.

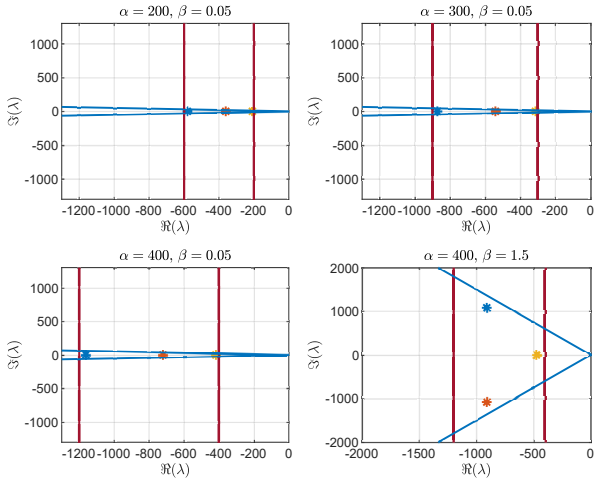


Fig. 5: Poles of the closed loop system.

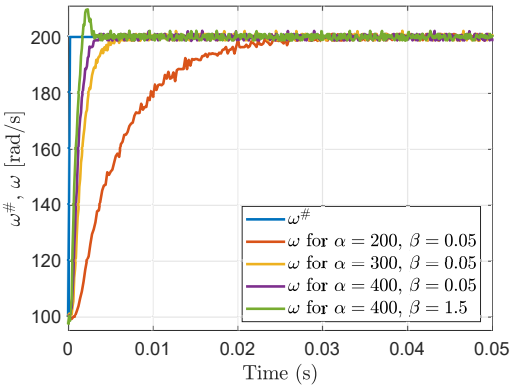


Fig. 6: Speed response for different values of $(\alpha,\ \beta)$.

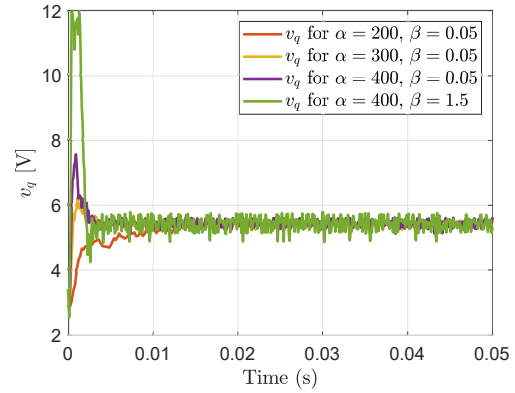


Fig. 7: Voltage transient for different values of $(\alpha,\ \beta)$.

## IV. Conclusions

This paper presents a practical approach to directly embedding advanced control methods, based on convex optimization, using microcontrollers. This enables advanced control laws to be regularly updated or recomputed without the need for external intervention. The practicality of this method has been shown in experimental tests. The method proposed in this paper is based on the regional pole placement, but this is only an example of what is possible, once the practice of embedding a simple, efficient solver is established. As further developments, we foresee the implementation of other advanced methods, like constrained $H_2$ or $H_\infty$ [16], or guaranteed cost control [17]. All of this should contribute to the effort of finding the best energy efficient controllers for tomorrow's electrical mobility.

## References


[1] Q. Huang, Q. Huang, H. Guo, and J. Cao, "Design and research of permanent magnet synchronous motor controller for electric vehicle," *Energy Science & Engineering*, vol. 11, no. 1, pp. 112–126, 2023.

[2] C.-Y. Chen, C.-H. Hsu, S.-H. Yu, C.-F. Yang, and H.-H. Huang, "Cascade PI Controller Designs for Speed Control of Permanent Magnet Synchronous Motor Drive Using Direct Torque Approach," in *(ICICIC)*, pp. 938–941, Dec. 2009.

[3] M. Tian, H. Cai, W. Zhao, and J. Ren, "Nonlinear Predictive Control of Interior Permanent Magnet Synchronous Machine with Extra Current Constraint," *Energies*, vol. 16, p. 716, Jan. 2023.

[4] D. H. Ha and R. Kim, "Nonlinear Optimal Position Control with Observer for Position Tracking of Surfaced Mounded Permanent Magnet Synchronous Motors," *Applied Sciences*, vol. 11, p. 10992, Jan. 2021.

[5] A. W. Depenbrock, "Field-oriented control of induction motors," in *Proceedings of the 24th IEEE Conference on Decision and Control*, pp. 1298–1303, IEEE, 1985.

[6] M. Chilali, P. Gahinet, and P. Apkarian, "Robust pole placement in LMI regions," *IEEE transactions on Automatic Control*, vol. 44, no. 12, pp. 2257–2270, 1999.

[7] B. H. d. Silva, P. S. Almeida, G. M. Soares, P. G. Barbosa, V. F. Montagner, and P. M. d. Almeida, "Universal-input integrated LED driver with robust $$\mathcal {H}_\infty $$controller for full-range high power factor and dimming capabilities under low current ripple," *Electrical Engineering*, Mar. 2023.

[8] M. Hypiusová and D. Rosinová, "Discrete-time pole-region robust controller for magnetic levitation plant," *Symmetry*, vol. 13, no. 1, 2021.

[9] S. Hassaine, B. Sari, S. Moreau, and B. Mazari, "Rapid prototyping of a multivariable control with pole placement by state feedback of a PMSM: LMI approach," in *IECON 2012*, pp. 1970–1975, Oct. 2012.

[10] R. H. Park, "Two-reaction theory of synchronous machines generalized method of analysis-part I," *Transactions of the American Institute of Electrical Engineers*, vol. 48, pp. 716–727, July 1929.

[11] M. Bodson, J. Chiasson, R. Novotnak, and R. Rekowski, "High performance nonlinear control of a permanent magnet stepper motor," vol. 1, Oct. 1992. Control Systems Technology,515 vol.1.

[12] K. Ogata, *Modern control engineering*. Prentice Hall, 5th ed., 2010.

[13] L. Vandenberghe and V. Balakrishnan, "Algorithms and software for LMI problems in control," *IEEE Control Systems Magazine*, vol. 17, no. 5, pp. 89–95, 1997.

[14] R. Delpoux, M. Bodson, and T. Floquet, "Joint Identification of Stepper Motor Parameters and of Initial Encoder Offset," *IFAC Proceedings Volumes*, vol. 45, no. 16, pp. 763–768, 2012.

[15] R. Delpoux, L. Kerhuel, and V. Léchappé, "On Chip Rapid Control Prototyping for DC motor," *J3eA*, vol. 20, pp. 1, rcp.ctrl–elec.fr/, 2021.

[16] M. Chilali and P. Gahinet, "H/sub /spl infin// design with pole placement constraints: an LMI approach," *IEEE Transactions on Automatic Control*, vol. 41, pp. 358–367, Mar. 1996.

[17] I. Petersen and D. McFarlane, "Optimal guaranteed cost control and filtering for uncertain linear systems," *IEEE Transactions on Automatic Control*, vol. 39, pp. 1971–1977, Sept. 1994.